International Orthopaedics (SICOT)
DOI 10.1007/s00264-017-3464-8

ORIGINAL PAPER

P15 peptide stimulates chondrogenic commitment and endochondral ossification

Jun Zhang[1,2] · Peter Eisenhauer[3] · Oz an Kaya[4] · Alexander R. Vaccaro[1,3] · Carol Diallo[1] · Andrzej Fertala[1] · Theresa A. Freeman[1]

Received: 10 November 2016 / Accepted: 22 March 2017

Abstract
Purpose The synthetic 15 amino acid biomimetic peptide sequence (P15) derived from a region of the alpha (α)-1 chain of collagen I, has been shown to promote α2 integrin activation and enhance intramembranous ossification. In this study, we ask if the P15 peptide also enhances bone formation through endochondral ossification, and determine if direct binding of α2 integrin with P15 mediates integrin activation.
Methods Mesenchymal cells (C3H10T1/2) were cultured in chondrogenic media and the expression of chondrogenic markers and integrin activation was determined by Western blot and fluorescent immunohistochemistry. A biosensor assay was used to determine if binding occurred between P15 and α2 β1 integrin. Finally, an *in vivo* model of endochondral ossification was used to determine the effect of P15 on bone formation.
Results In the presence of P15, chondrogenesis and activation of α5 integrin were enhanced, as observed by both Western blot analysis and immunoflourescent staining. A biosensor assay investigating the specificity of the interaction between P15 with α2β1 integrin determined direct binding does not occur. When P15 was added to Matrigel implanted in a murine endochondral ossification model, in the presence of bone morphogenic protein-2 (BMP-2), a significant increase in chondrocyte differentiation and mineralization was observed.
Conclusion P15 does not directly activate integrins by binding, but does upregulate integrin signaling to enhance differentiation of both osteoblasts and chondrocytes to increase both intramembranous and endochondral bone formation.

Keywords P15 peptide · MicroCT analysis · Chondrogenesis · Endochondral ossification · Bone density · Integrin · Collagen

Introduction

Spinal fusion surgery is one of the most commonly performed procedures in the United States [1]. Successful healing of the fusion requires rapid bone deposition and turnover [2–4]. One critical factor that influences the rate of osteogenesis is the interaction between surface receptors of bone forming cells and specific motifs of collagen I, the most prevalent extracellular matrix (ECM) protein [5–7]. The P15 peptide sequence (GTPGPQGIAGQRGVV), derived from residues 766–780 of the alpha (α) chain of collagen I, can serve as a cell binding domain [8]. Multiple studies have shown that P15 enhances fibroblast and osteoblast attachment and proliferation and promotes matrix production [8–11]; likewise, a number of reports detail the ability to enhance bone formation [8, 12, 13]. Currently, P15 adsorbed to anorganic bone matrix (P15/ABM) is undergoing clinical trials, as an agent to enhance ossification in spinal fusion surgery [14].

Current strategies to promote fusion vertebrae and repair of non-unions include the placement of allograft bone, autologous bone, and/or bone morphogenic protein (BMP) in the fusion space [15, 16]. The use of autologous or allograft bone lends stability while BMP stimulates ossification to enhance bone

✉ Theresa A. Freeman
Theresa.freeman@jefferson.edu

1 Sidney Kimmel Medical College Department of Orthopaedic Surgery, Thomas Jefferson University, 501 Curtis Bldg., 1015 Walnut St., Philadelphia, PA 19107, USA

2 Orthopaedic Medical Center, 2nd Hospital of Jilin University, 218 Ziqiang Street, Changchun 130041, People's Republic of China

3 Rothman Institute at Jefferson, 925 Chestnut Street, Philadelphia, PA 19107, USA

4 Department of Orthopedics and Traumatology, Istanbul University, Istanbul 34093, Turkey

Published online: 08 April 2017

formation during the fusion process. However, problems exist with each of these solutions. Using autologous bone results in a faster fusion rate compared to allograft bone, but the harvesting of autologous bone can have unfavourable complications [17–19]. The clinical use and cost-effectiveness of BMPs is also currently under debate, as ectopic bone formation and tissue inflammation can occur due to leakage into other tissue areas (spinal canal/foramen) [20, 21]. Thus, finding a solution which both lends stability and support while promoting enhanced bone formation is still under investigation. One solution that is being tested to address this need is *i*-FACTOR, a novel bone graft substitute composed of P15 adsorbed to the anorganic bone material (ABM) that is in clinical trials for use in anterior lumbar inter-body fusion. The premise is that P15 will stay attached to the anorganic bone decreasing the likelihood of release into the local environment [14]. Additionally, facilitation of bone formation by P15 is much different than BMPs, which are growth factors that can stimulate many biological processes, in addition to bone formation.

To date, several studies have reported that the P15 peptide enhances osteogenic differentiation and bone formation by increasing cell attachment and matrix production through a putative interaction with α2β1 [8, 22, 23]. However, the effect of P15 on chondrogenic differentiation and endochondral bone formation, which can also be stimulated by integrin interactions, has not been investigated. In this report, we show chondrogenesis and endochondral bone formation is increased in the presence of P15, both *in vitro* and *in vivo* (when BMP2 is present). Analysis of α5 integrin activation also showed an increase during chondrogenesis when in the presence of P15. Finally, the use of biosensor technology definitively shows that there is no direct binding between P15 and integrin α2β1 integrin. Taken together, this data indicates the probable mechanism of action of P15 is to enhance cell attachment and nonspecifically activate integrin signaling to enhance both intramembranous and endochondral ossification. This is clinically relevant, as bone formation during bone repair and fusion of non-unions can be mediated by both intramembranous and endochondral ossification [24].

Methods

Cell culture

The murine MSC line, C3H10T1/2 (ATCC (CCL-226), Manassas, VA) was cultured in Dulbecco's modified Eagle's medium (DMEM; Cellgro, Mediatech, Manassas, VA) with 5% fetal bovine serum (Invitrogen, Carlsbad, CA; Life Science Technologies) and 5% fetal calf serum (Invitrogen, Life Science Technologies) with 100 U/(ml of media) penicillin (Cellgro) and 100 μg/(ml of media) streptomycin (Cellgro), in 5% CO2 at 37 °C. C3H10T1/2 cells at passages 6 and 14 were used for all experiments. The cells (8×10^4) were seeded in culture dishes (BD Biosciences, San Jose, CA) on either air-dried P15 peptide (Cerapedics, Denver, CO) or untreated tissue culture plastic. To induce maturation, cells were incubated in chondrocytic differentiation media (DMEM with 10% FBS, dexamethasone (0.1 mM, Sigma), ascorbate (0.17 mM, Sigma), 1% Insulin, Transferrin and Selenium (ITS) Premix (BD Biosciences, San Jose, CA), and transforming growth factor-β (TGF-β; 10 ng/ml, R&D, Minneapolis, MN)). Untreated cells were maintained as an immature phenotype and served as a control. Media was changed every 2 days up to 13 days and cultures collected at day (D) 6 and D13 for analysis. All the cultures were kept at 37 °C in a humidified atmosphere of 5% CO_2.

Immunohistochemical analysis

For immunohistochemistry, cells seeded on culture dishes with or without P15 peptide coating were either grown on chamber slides or cytospun onto slides after D13 of chondrogenic culture. PFA fixed cells were washed three times with PBS then incubated with blocking solution for 2 h at room temperature. Subsequently, cells were incubated overnight at 4 °C with the following primary antibodies (1:50 : α5 integrin (Chemicon-Millipore, Jaffrey, NH), phosphorylated Focal Adhesion Kinase-Tyr397 (pFAK; 1:50) (Santa Cruz Biotech, Santa Cruz, CA), runt-related transcription factor-2 (RUNX2; 1:100), matrix metalloproteinase-13 (MMP13; 1:200) (Cemines Inc, Golden, CO), vascular endothelial growth factor (1:100; VEGF), and type X collagen (COLX; 1:100) (Southern Biotech Associates Inc, Birmingham, AL). After three PBS washes, cells were incubated for 1 h at room temperature with fluorescently labeled secondary antibodies (1:200): Alexafluor 594 anti-rabbit and 488 anti-mouse (Molecular Probes, OR). Unbound secondary antibodies were washed 3X with PBS and the slide was mounted with Vectashield hardset with DAPI (Vector Labs, Burlingame, CA) for microscopic imaging.

Protein extraction and western analysis

Cells were washed at D13 with PBS, and centrifuged for five minutes at 2000×*g* in ice-cold PBS. The supernatant was removed and the pellet was resuspended in lysis buffer and centrifuged for 15 minutes at 14,000×*g*; the supernatant was removed and stored at −80 °C. Approximately 40 μg of protein was loaded onto an SDS polyacrylamide gel, and after electrophoresis the proteins were transferred to a PVDF membrane (Immobilon, Millipore, USA) in buffer (TG Buffer with 20% methanol) for two hours 30 minutes at 4 °C. The membrane was blocked in Tris-buffered saline and Tween 20 (TBST) with 2% electro-chemiluminescence (ECL) buffer (Amersham, Piscataway, NJ) for one hour with shaking. The membranes

were then incubated with their respective primary antibodies (MMP13, COLX, VEGF) in TBS with 0.05% Tween 20 and 2% ECL buffer overnight at 4 °C. The blots were washed three times in TBST and the secondary antibodies (Santa Cruz Biotechnology, USA) were applied for one hour at room temperature. After washing with TBST, the membrane was placed in an ECL advanced detection system (Amersham) for five minutes at 25 °C. Protein detection was performed using a Fujifilm Intelligent Dark Box (Fujifilm Company).

Murine subcutaneous heterotopic ossification model

All animal procedures were conducted under the approval of the Thomas Jefferson University Institutional Animal Care and Use Committee. P15 peptide and recombinant human Bone Morphogenic Protein-2 (BMP2) (Invitrogen, Life Science Technologies, Carlsbad, CA) were used as chemical stimulators of bone growth. After receipt from vendor, male CD-1 mice (Charles Fischer Labs, Wilmington, MA) aged eight to ten weeks were allowed to acclimatize to the new animal facilities for two days. Two experiments were conducted with different treatment conditions, but the same protocol. The first experiment compared the effect of P15 with that of BMP2. Separate aliquots of Matrigel (BD Biosciences) were prepared (250 μl) and mixed with either BMP2 or P15 (1.25 μg/ml and 2.50 μg/ml, final concentration). Separate aliquots were injected subcutaneously into the ventral abdominal region of the mice. The animals received two injections of Matrigel with BMP2 in the right hypochondriac and right iliac region and two injections of Matrigel with P15 in the left hypochondriac and left iliac region, respectively. A second experiment with another group of mice compared the effect of BMP2 with that of P15 + BMP2. For this experiment, separate aliquots of Matrigel were prepared (250 μl) and mixed with either BMP2 (1.25 μg/ml) alone or in combination with P15 (1.25 μg/ml). These aliquots were injected subcutaneously into the ventral abdominal region of the mice. Matrigel solidifies at 37 °C to form a localized source of BMP2 or P15 or P15 + BMP2 (depending upon treatment). The solidified gels are easily distinguished from surrounding tissues and a well-defined plug between skin and muscles is easily excised for preparation of histological sections. Experiments were run in triplicates. Subjects were observed daily for any ill effects and were euthanized by asphyxiation in CO_2 at D8 (second experiment only), D12 (first and second experiment) and 20 (second experiment only) after injections. The transplanted masses were excised and analyzed by microCT (Scanco μCT, Basserdorf, Switzerland) and histology.

MicroCT analysis

Transplanted masses were excised, fixed in 4% PFA, and subjected to microCT analysis (Scanco μCT 40; Basserdorf, Switzerland) as previously described [25]. The scans were performed using an X-ray tube energy of 45kVp, a current of 177 μA and a 200-ms integration time producing a spatial resolution of 12 μm3 voxel size. Each mass was traced and a contour was created and evaluated for bone volume fraction (BV/TV), i.e., the ratio of bone volume over total volume. The 3D data sets were low-pass filtered using a Gaussian filter ($\sigma = 0.80$, support = 1) and segmented with a fixed threshold filter (160 mg HA/cm3). Values collected for BV/TV are represented as percentages to control for both variation in the size of the Matrigel mass and variation between individual mice. Each mouse was injected with four Matrigel masses, which always included an untreated BMP-2 positive control which represented the best (100%) response within each mouse. Treatments were then compared to the best (100%) response to the BMP-2 control in each mouse and the percent difference was determined.

Matrigel mass histology

For histological analyses, matrigel masses from at least four ($n = 3$) different mice were collected, embedded in paraffin, and sectioned at 6 μm thick for each condition (control, μsp, and both nsp-DBD treatments). From each collected matrigel sample, multiple sections from different regions were obtained. The slides were deparaffinized, rehydrated, and stained with haematoxylin and eosin (H&E) and Alcian blue (1%, 8GX, Sigma Aldrich; cartilage) or Vectashield HardSet with DAPI (Vector Labs, Burlingame, CA; count cells).

Image acquisition and analysis

Imaging was performed using a Nikon E800 (Nikon, Melville, NY) with a Retiga EXi digital cooled charge-coupled device camera with RGB electronic filter (QImaging, Surrey, BC, Canada) or on a Nikon Optiphot with an RT-Spot camera (Diagnostic Instruments, Sterling Heights, MI). All images in each group were exposed using the same settings. Image quantitation was performed with Image Pro Plus software (Media Cybernetics, Silver Spring, MD).

P15 interaction with $\alpha 2\beta 1$ integrin

A biosensor (Sensiq Pioneer, SensiQ Technologies, Inc.) was employed to analyze P15-$\alpha 2\beta 1$ integrin binding interactions. For these assays, a biotinylated form of the P15 peptide was employed to facilitate its binding to the surface of a sensor chip (GenScript, Inc.). In brief, neutravidin (Thermo Scientific, Waltham, MA), an avidin variant, was first bound to the chip surface (COOH1 SPR Chip, SensiQ Technologies, Inc.); carboxylate groups present on the surface were activated by injection of a 1:1 mixture of 0.1 M N-hydroxysuccinimide and 0.4 M N-Ethyl-3-(3-dimethylaminopropyl) carbodiimide (Thermo Scientific,

Waltham, MA). Subsequently, 100 μg/ml nutravidin in 10 mM acetate buffer at pH 4.5 was allowed to bind to the activated surface until a response plateau was reached. The residual active groups were blocked by an injection of 100 μL of 1 M Tris-HCl (pH 8.5). After re-equilibration with 4-(2-hydroxyethyl)-1-piperazineethanesulfonic acid (HEPES)-buffered saline containing 0.005% of Tween 20 (HBS-TE), the nutravidin-coated chip bound the biotinylated P15 (10 nM) so as to saturate all available biotin-binding sites. Subsequently, non-specific binding sites were blocked by injecting a 1% solution of bovine serum albumin (BSA) dissolved in HBS-TE. Excess non-bound material was removed by washing the chip with HBS-TE, followed by three consecutive washes with 10 mM HCl.

To analyze the kinetic of P15-α2β1 integrin binding, in which the P15 served as an acceptor, an active recombinant variant of this integrin was employed (R&D Systems, Minneapolis, MN). A sensor chip with immobilized P15 acceptor was primed with HBS-TE supplemented with 1 mM of $MgCl_2$ and 1 mM $CaCl_2$ at 25 °C for ten minutes. Subsequently, the association phase was initiated by injecting a free integrin interactant at a rate of 10 μl/min for ten minutes. After that time, the dissociation phase was initiated by injecting the analyte-free buffer.

After each assay, the surface of the sensor chip was regenerated by washing with 10 mM HCl, followed by equilibration with HBS-TE supplemented with 1 mM of $MgCl_2$ and 1 mM $CaCl_2$. During regeneration cycles attention was paid to completely remove surface-bound analyte and the washing continued until a response equal to a baseline value was reached.

For binding assays, free integrin interactant was added at concentrations ranging from 3.5 nM to 225 nM. Data from the biosensor were analyzed by the global fitting method described by Myszka and Morton [26]. For each assay, the association rate constants (k*on*) and the dissociation rate constants (k*off*) were obtained, and the equilibrium dissociation constants (K*d*) values were calculated from a ratio of k*off*/k*on*.

Control binding assays

In addition to the P15-α2β1 integrin binding measurements, the following control assays were also performed: (1) α2β1 integrin binding analysis was carried out with collagen I (BD Biosciences) serving as an acceptor immobilized directly on a COOH1 chip. Collagen I-α2β1 integrin binding was performed as described for the P15–α2β1 integrin binding. (2) Native collagen I-α2β1 integrin binding in the presence of free 2 μM P15; here the P15 served as a potential competitor for the collagen I-α2β1 integrin binding. (3) P15-anti-P15 antibody binding assay; the accessibility of the nutravidin-bound P15 for the binding interactions was measured. The anti-P15 antibody, the P15 binding partner was added as a free analyte at concentrations ranging from 1.5 nM to 100 nM, (4) BSA-α2β1 integrin binding; for this control assay, the binding interactions between the immobilized BSA acceptor and free α2β1 integrin (3.5 nM to 225 nM) was analyzed. The flow rates and duration of the association and the dissociation phases in the above control groups were identical to those described for the P15- α2β1 integrin interaction.

Statistical analysis

Analysis was performed using a one-way analysis of variance. A level of significance (α), or a p-value of less than 0.05, with a 95% confidence interval was determined. Representative data are presented as the mean ± standard error of the mean from three or more independent analyses.

Results

P15 peptide enhances chondrocyte differentiation in vitro

Cells of a murine MCS cell line were cultured in dishes coated with or without the P15 peptide and chondrogenic differentiation was assessed. At D6, when compared with the uncoated control plates the P15 peptide cultured cells showed intense alkaline phosphatase and alcian blue staining, indicating deposition of chondrogenic differentiation and increased proteoglycan synthesis, respectively, (Fig. 1a). Western blot analysis at D13 indicated that there was a significant increase in the levels of runt-related transcription factor-2 (RUNX2), matrix metalloproteinase-13 (MMP13), vascular endothelial growth factor (VEGF), and collagen X (COLX) proteins ($p < 0.05$) (Fig. 1b). Increased expression of RUNX2, COLX, and MMP13 was also confirmed by immunofluorescent staining (Fig. 1c). Taken together, these results demonstrated the ability of P15 peptide to enhance C3H10T1/2 cells commitment to the chondrocyte lineage.

P15 increases α5 integrin expression and activates pFAK signaling

To determine if P15 enhances chondrogenic differentiation through integrin α5/pFAK signaling, we stained cells that had been maintained on either uncoated or P15-coated dishes using antibodies specific for α5 integrin (green) or pFAK (red). Six hours after plating, cells grown on P15-coated plates exhibited greater numbers of filapodia with increased amounts of yellow fluorescence indicating P15 activation of this pathway (colocalization of pFAK with α5 integrin; high mag. in inset; Fig. 1d). Protein lysates of cells grown on P15 surface from the six hour time point were also analyzed by Western blot and showed increased levels of pFAK and α5 integrin proteins (Fig. 1e). Quantitation of Western blot band density is shown in Fig. 1f ($p < 0.05$).

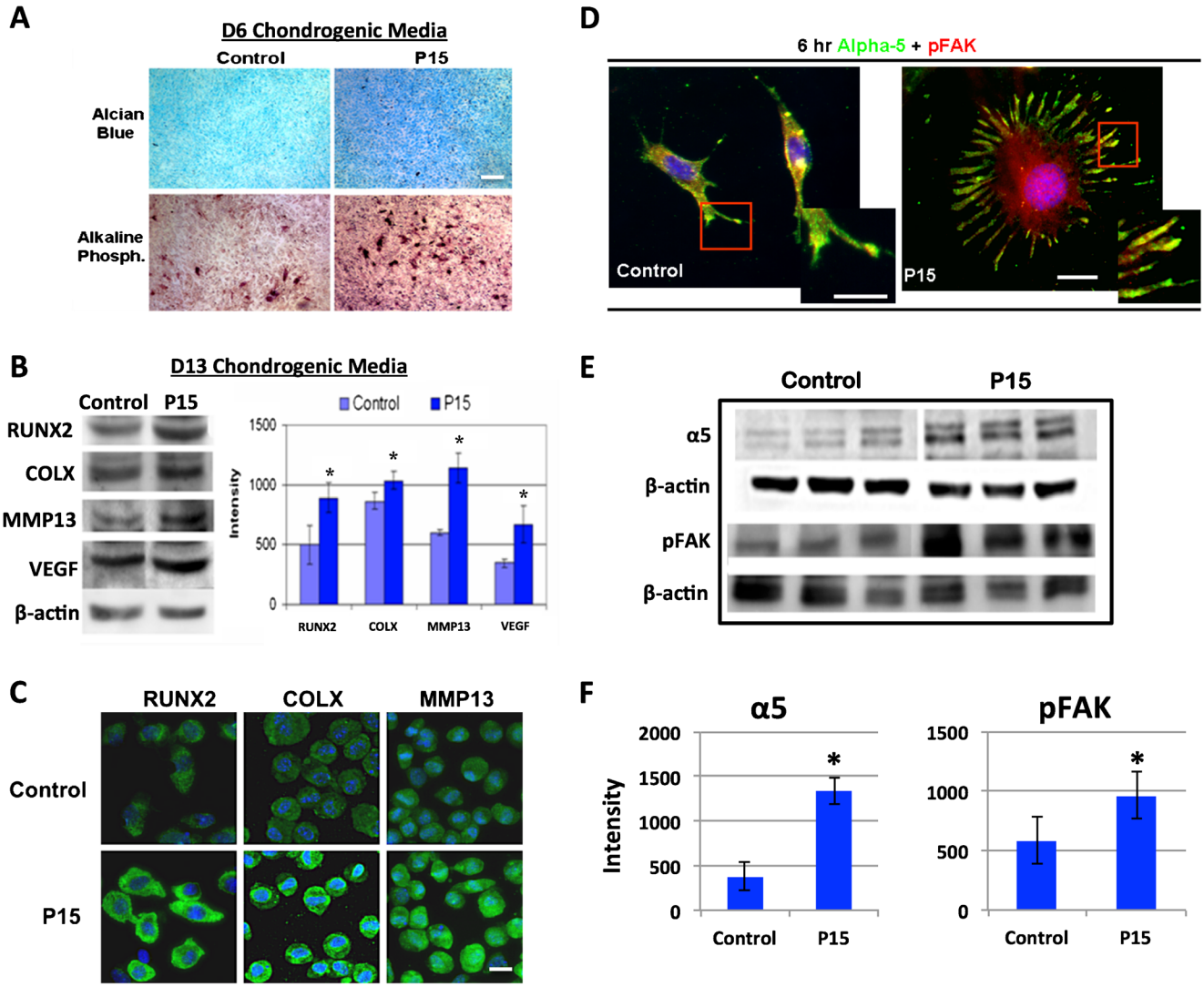

Fig. 1 P15 enhances chondrogenic differentiation and integrin signaling. **a** Murine MSC cells differentiated for six days in chondrogenic culture media show increased alcian blue (proteoglycan) and alkaline phosphatase (chondrogenic maturation) staining (mag. bar = 500 mm; $n = 3$). **b** Western blot shows increases in chondrogenic marker proteins in cells grown on P15 coated dishes at D13 in chondrogenic media ($n = 3$, $^*p < 0.05$). **c** Representative image with immunofluorescent staining confirms western blot results (mag. bar = 100 mm). **d** Representative image of cells plated on P15-coated dishes show increased spreading, filopodia, attachment and colocalized staining for α5 integrin and pFAK as compared with control (mag. Bar = 10 mm). **e** Western blot analysis confirms increases in α5 integrin and pFAK proteins from cells grown on P15-coated dishes. β-actin staining used to control for differences in total protein concentration. **f** Graphs showing quantitation of intensity of Western blot staining shows increased α5 integrin and pFAK proteins from cells grown on P15-coated dishes $^*(p < 0.05, n = 3)$

P15 alone does not direct endochondral ossification in vivo

We used a subcutaneous heterotopic ossification model to determine whether P15 could independently direct endochondral bone formation. For this study, we compared bone formation in Matrigel matrix containing either P15 or BMP2 ($n = 4$; Fig. 2a). MicroCT analysis indicated that at D12 there was no bone formation in the Matrigel-P15 implant; in contrast, the Matrigel-BMP2 matrix displayed consistent bone formation (Fig. 2b). To ascertain if the failure of Matrigel-P15 to induce bone formation was due to impaired cell migration, we counted the number of DAPI positive cells in both Matrigel preparations at two concentrations of P15 and BMP2: 1.25 μg/ml and 2.50 μg/ml final concentration (Fig. 2c). By D12, when BMP2 was compared with P15, no differences were observed in the numbers of cells that had migrated into the Matrigel at either concentration (Fig. 2d).

P15-BMP2 increases chondrocyte differentiation and enhances early endochondral ossification.

To test whether P15 could enhance BMP-dependent bone formation, we compared Matrigel-BMP2 with Matrigel-P15 + BMP2 masses (P15 – 1.25 μg/ml, BMP2 – 1.25 μg/ml).

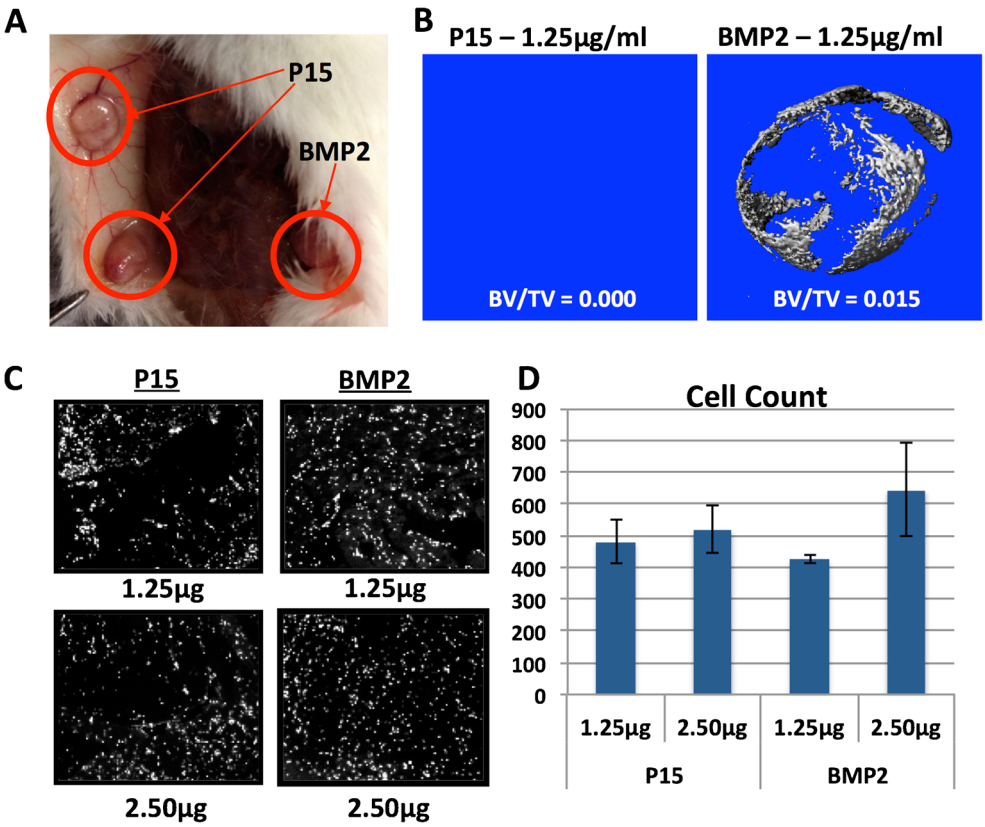

Fig. 2 P15 does not independently direct endochondral ossification *in vivo*. **a** In situ gross pathology image of subcutaneous Matrigel masses with either P15 or BMP2 at day 12 post injection. **b** MicroCT 3-dimensional image of mineralized masses show no bone formation in P15 masses, but normal bone formation in BMP2 masses. **c** DAPI stained sections of P15 and BMP2 matrigel masses show no difference in cell invasion into Matrigel. **d** Graphic quantitation of cells in 5 mm^2 areas of P15 and BMP2 masses show no difference in cell invasion ($n = 4$)

Alcian blue staining showed that cartilage had formed within the masses at an early time point before significant bone deposition (D8; Fig. 3). Compared to BMP2, at D8 the P15 + BMP2 Matrigel matrix exhibited significantly greater amounts of cartilage (Fig. 3, $p < 0.05$). At D12 and D20, scanning was performed to determine the degree of mineralization (Fig. 3). At D12, microCT analysis of P15 + BMP2 matrix indicated that there was a 64% increase in mineralization compared to masses containing BMP2 alone (Fig. 3, $p < 0.05$). By D20, regardless of treatment, microCT analysis showed equivalent amounts of mineralization (Fig. 3).

P15 does not directly bind to α2β1 integrin

To elucidate the mechanism by which P15 activated cells, a biosensor technology was utilized (see diagram, Fig. 4a). As indicated in Fig. 4b, no specific P15-α2β1 integrin binding was recorded. In contrast, a binding interaction between collagen I and α2β1 integrin was characterized by k_{on} of 1.23×10^4 ($M^{-1}s^{-1}$) and k_{off} of 9.99×10^{-4} (s^{-1}) (Fig. 4c). The corresponding K_d value for this interaction was 81.2 nM. To further confirm the lack of P15-α2β1 integrin binding interaction, we employed an assay in which the P15 peptide was a competitor for the collagen I-α2β1 integrin binding. As demonstrated in Fig. 4d, the presence of P15 did not change collagen I-α2β1 integrin binding characteristics. In these assays, the kinetic parameters of collagen I-α2β1 integrin interaction were similar to those calculated for a corresponding interaction performed in the absence of the P15 inhibitor. Specifically, the following values were calculated: k_{on} of 1.21×10^4 ($M^{-1}s^{-1}$), k_{off} 1.29×10^{-3} (s^{-1}), and corresponding K_d of 107 nM. Because the α2β1 integrin was still able to bind to the collagen I target, these data indicate that free P15 competitor did not interact with the α2β1 integrin in solution.

The accessibility of nutravidin-immobilized P15 peptide for binding free interactants was confirmed by its ability to bind anti-P15 antibody. As demonstrated in Fig. 4e, this antibody bound P15 strongly with a K_d value of 8.9 nM. In addition, the lack of BSA-α2β1 integrin binding (Fig. 4f) further indicated the specificity of measured interactions. Finally, we determined if P15 bound to fibronectin or BSA could indirectly activate integrins. Again, no binding was observed between BSA or fibronectin and P15 (Fig. 4g and h).

Discussion

P15 has been shown in many studies to facilitate bone production by modulation of cell binding, migration, proliferation, and differentiation, in addition to promoting synthesis and secretion of extracellular matrix [27, 28]. In this report, we further investigated the mechanism of action of P15's

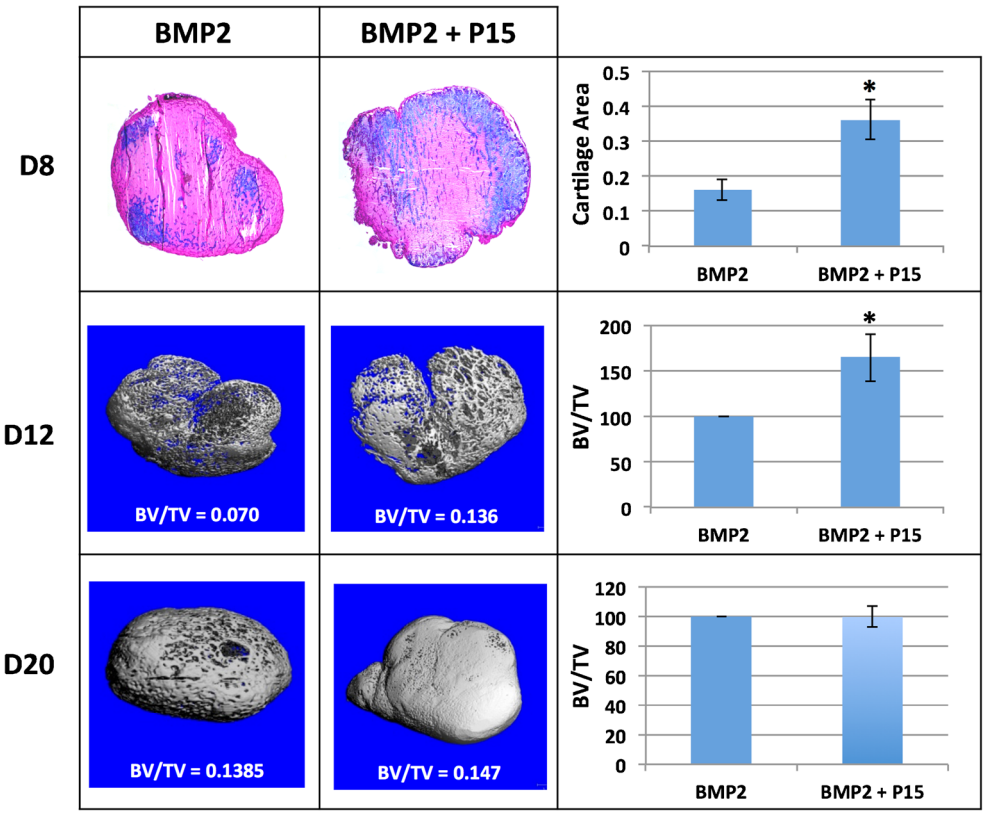

Fig. 3 P15 + BMP2 enhances chondrogenesis and endochondral ossification compared to BMP2 alone. Alcian blue staining of BMP2 and BMP2 + P15 at D8 show increased cartilage regions in BMP2 + P15 masses. Quantitation of alcian blue staining area show significantly greater cartilage is present in BMP2 + P15 masses. MicroCT 3D imaging of mineralized masses show greater bone formation in BMP2 + P15 masses at D12, but no difference at D20. Analysis of BV/TV at D12 show a 64% increase in bone formation BMP2 + P15 masses relative to BMP2 controls, however no differences in bone formation were seen at D20. *($p < 0.05$), $n = 5$ for cartilage, $n = 4$ for D12 and 20 BV/TV

putative, direct binding to α2β1 integrin and determined if the P15 peptide could interact with α5 integrin to promote chondrogenesis and bone formation via endochondral ossification. Based on our previous report showing enhanced osteogenesis by P15 activation of α2 integrin and FAK [8], we asked whether P15 could similarly activate integrin α5 to promote stromal cell commitment and enhanced chondrogenesis [29]. We further tested the efficacy of the P15 peptide *in vivo* in a mouse model of heterotopic ossification.

Many past studies have detailed the effectiveness of P15 in enhancing bone formation and reported that the osteogenic activities of P15 are mediated through activation of the collagen-selective integrin α2β1 [9–11]. The ability of the α2β1 integrin to upregulate osteoblastic differentiation and matrix mineralization has been well described [30, 31]. Results from this study confirmed P15 also increased α5 integrin signaling and the expression of protein markers of chondrogenic differentiation. Specifically, we showed that mesenchymal cells grown *in vitro* on surfaces coated with the P15 peptide have increased α5 integrin expression and show activation of FAK. When placed in chondrogenic media, cells grown on P15-coated dishes showed intense alkaline phosphatase and alcian blue staining. Western blot analysis confirmed expression of the chondrocyte markers RUNX2, COLX, MMP13, and VEGF were all elevated. Thus, *in vitro*, the P15-α5 integrin response mimicked the increased α2 integrin signaling previously reported to promote osteogenesis [8].

To determine if the interaction of the P15 peptide with α2 integrin was direct binding, we assessed this using biosensor analysis. The fact that no specific P15-α2β1 integrin binding was observed strongly suggested that activation of P15 with integrins is more likely to be indirect and not direct binding of P15 with the integrin. This finding was a bit surprising, as this peptide was derived from a region of the collagen I molecule involved in integrin binding. However, it should be noted that a limitation of the biosensor assay is when P15 is immobilized to streptavidin it is assessed as a linear peptide. Thus, the structure required for binding interactions may be lacking. In its native state P15 is part of the collagen triple helix and the specificity of the helical arrangement is needed for all known collagen interactions. Therefore, we cannot rule out the potential that P15 activity, as observed when formulated with hydroxyapatite, as in iFactor, may be the result of the specific structure assumed when bound to the hydroxyapatite material. It is predicted that the interaction of P15 with hydroxyapatite fixes the structure in a favorable position that may resemble this peptide in its native form, i.e., the collagen triple helix.

Further investigation to determine whether P15 could independently direct chondrogenesis or mineralization *in vivo* using a mouse heterotopic ossification model determined that in the absence of BMP2, mesenchymal cells would indeed migrate into the Matrigel, but would not differentiate into chondrocytes. When P15 was combined with BMP2 in the Matrigel, it was observed that an increased number of

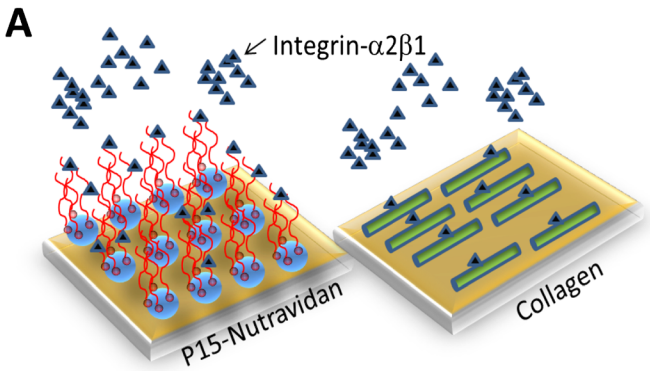
A
Integrin-α2β1
P15-Nutravidan
Collagen

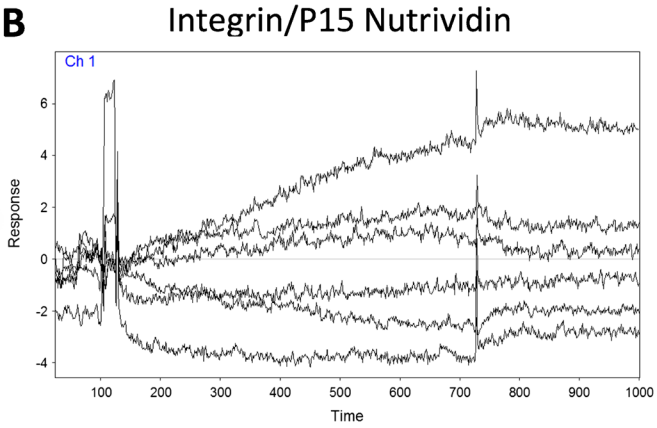
B
Integrin/P15 Nutrividin
Ch 1
Response
Time

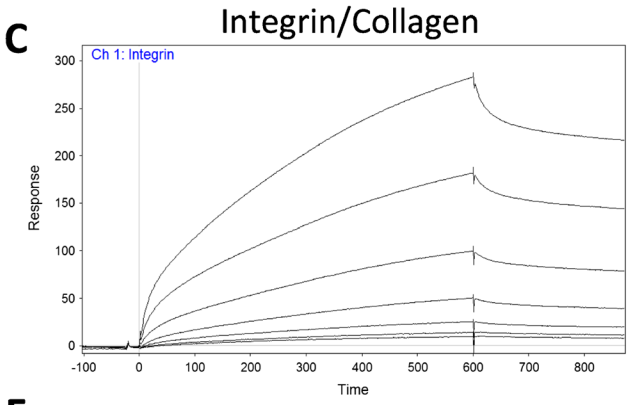
C
Integrin/Collagen
Ch 1: Integrin
Response
Time

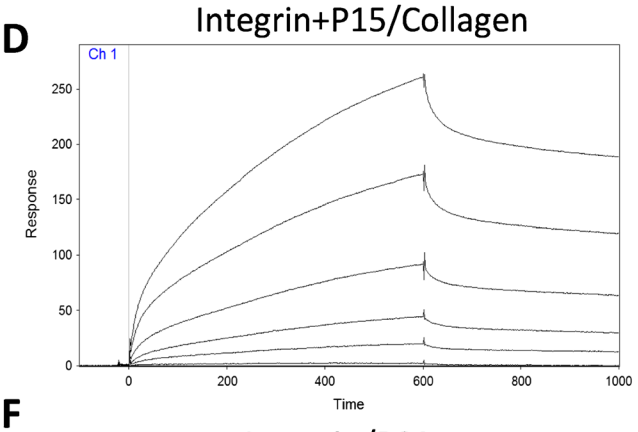
D
Integrin+P15/Collagen
Ch 1
Response
Time

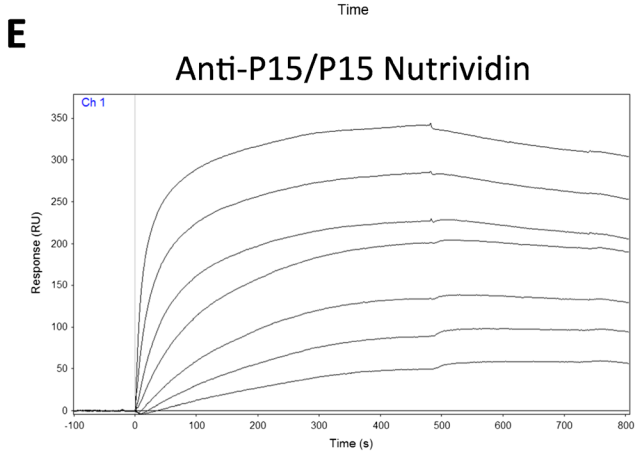
E
Anti-P15/P15 Nutrividin
Ch 1
Response (RU)
Time (s)

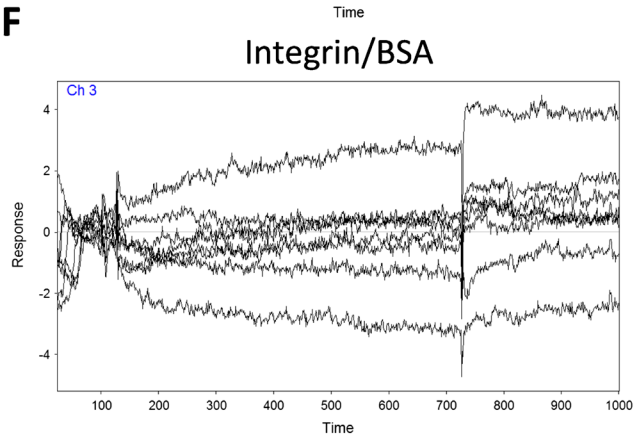
F
Integrin/BSA
Ch 3
Response
Time

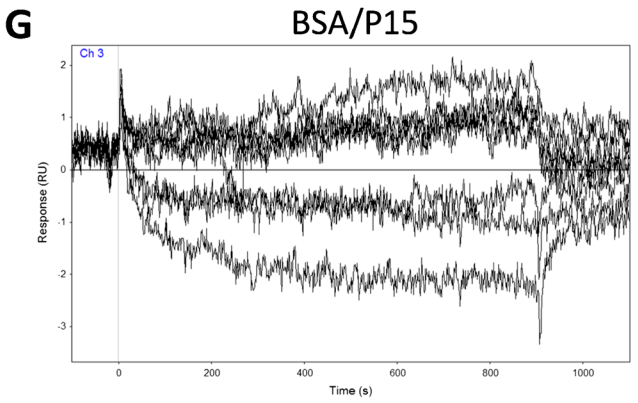
G
BSA/P15
Ch 3
Response (RU)
Time (s)

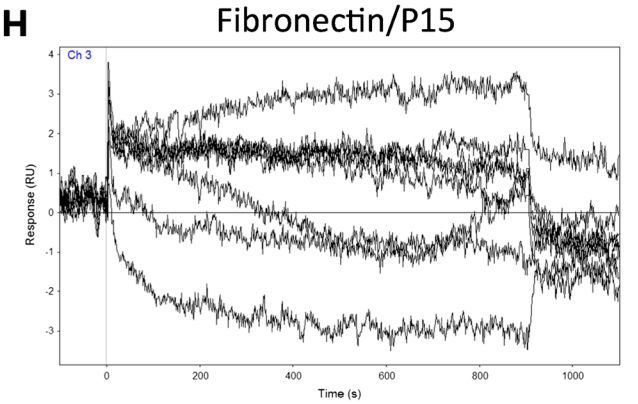
H
Fibronectin/P15
Ch 3
Response (RU)
Time (s)

◀ **Fig. 4** P15 does not directly bind α2β1. **a** Illustration of the experimental design of biosensor binding assays; left panel depicts a sensor coated with biotinylated P15 peptide while the right panel shows a control sensor coated with collagen I. **b** Graphic representation of P15-α2b1 integrin binding interaction shows no detectable interaction. **c** Graphic representation of collagen I-α2b1 integrin interaction shows a strong interaction. **d** Collagen I-α2b1 integrin interaction in the presence of 2 mM of free P15 shows a strong interaction. **e** P15-anti-P15 antibody binding assays demonstrating the availability of nutravidin-immobilized P15 to interact with free analytes. Control **f** BSA-α2β, **g** BSA-P15, and **h** Fibronectin-P15 integrin binding assays show no detectable interactions

mesenchymal cells transformed into chondrocytes at earlier time points (Fig. 3). In addition, an increase in chondrogenesis at D8 and endochondral bone formation at D12 was observed. Even though increased bone was observed at D12, by D20 the bone produced was equivalent to that of BMP2 alone.

As the results from the bioassay clearly ruled out the possibility of a direct interaction of P15 with α2β1, we believe it is possible that a third molecule may be required to interact with P15 to facilitate the interaction with integrins and enhance differentiation of both osteoblasts and chondrocytes. Taken together, these results indicate that although the P15/integrin interaction is not direct or specific, the enhancement of integrin signaling by P15 acts to drive multipotential stromal cells toward differentiation. In the presence of BMP2, and other growth factors, the determination of which lineage (osteogenic or chondrogenic) to differentiate depends on the environmental conditions. Thus, P15 may serve to increase the attachment of mesenchymal cells to the matrix and then in response to BMP2/growth factors, leads to increased chondrogenic differentiation and an earlier start to endochondral bone formation. This report supports the view that P15 is valuable for enhancing not only intramembranous ossification, as previously reported, but also endochondral ossification, thus increasing the value of this peptide for clinical use.

ABM, Anorganic bone matrix; BMP, Bone morphogenic protein; BSA, Bovine serum albumin; BV/TV, Bone volume fraction; C3H10T1/2, Murine mesenchymal stem cell line; COLX, Type X Collagen; ECM, Extracellular matrix; MMP13, Matrix metalloproteinase-13; pFAK, phosphorylated focal adhesion kinase; RUNX2, Runt-related transcription factor-2; VEGF, Vascular endothelial growth factor.

Acknowledgements We thank Dr. Irving Shapiro for his valuable discussions and manuscript revisions.

Compliance with ethical standards

Conflicts of interest No conflicts of interest exist for Jun Zhang, Peter Eisenhauer, Ozcan Kaya, Carol Diallo, Andrzej Fertala, or Theresa A Freeman.

Funding This work was funded by Cerapedics, Inc.

Animal rights All animal procedures were conducted under the approval of the Thomas Jefferson University Institutional Animal Care and Use Committee.

References

1. Deyo RA, Gray DT, Kreuter W, Mirza S, Martin BI (2005) United States trends in lumbar fusion surgery for degenerative conditions. Spine 30(12):1441–1445, discussion 1446-1447
2. Siu RK, Lu SS, Li W, Whang J, McNeill G, Zhang X, Wu BM, Turner AS, Seim HB 3rd, Hoang P, Wang JC, Gertzman AA, Ting K, Soo C (2011) Nell-1 protein promotes bone formation in a sheep spinal fusion model. Tissue Eng Part A 17(7-8):1123–1135. doi:10.1089/ten.TEA.2010.0486
3. Reid JJ, Johnson JS, Wang JC (2011) Challenges to bone formation in spinal fusion. J Biomech 44(2):213–220. doi:10.1016/j.jbiomech.2010.10.021
4. Nerubay J, Marganit B, Bubis JJ, Tadmor A, Katznelson A (1986) Stimulation of bone formation by electrical current on spinal fusion. Spine 11(2):167–169
5. Chang CF, Lee MW, Kuo PY, Wang YJ, Tu YH, Hung SC (2007) Three-dimensional collagen fiber remodeling by mesenchymal stem cells requires the integrin-matrix interaction. J Biomed Mater Res A 80(2):466–474. doi:10.1002/jbm.a.30963
6. Franceschi RT, Ge C, Xiao G, Roca H, Jiang D (2009) Transcriptional regulation of osteoblasts. Cells Tissues Organs 189(1-4):144–152. doi:10.1159/000151747
7. Myllyharju J, Kivirikko KI (2004) Collagens, modifying enzymes and their mutations in humans, flies and worms. Trends Genet 20(1):33–43. doi:10.1016/j.tig.2003.11.004
8. Liu Q, Limthongkul W, Sidhu G, Zhang J, Vaccaro A, Shenck R, Hickok N, Shapiro I, Freeman T (2012) Covalent attachment of P15 peptide to titanium surfaces enhances cell attachment, spreading, and osteogenic gene expression. J Orthop Res Off Publ Orthop Res Soc 30(10):1626–1633. doi:10.1002/jor.22116
9. Gomar F, Orozco R, Villar JL, Arrizabalaga F (2007) P-15 small peptide bone graft substitute in the treatment of non-unions and delayed union. A pilot clinical trial. Int Orthop 31(1):93–99. doi:10.1007/s00264-006-0087-x
10. Yang XB, Bhatnagar RS, Li S, Oreffo RO (2004) Biomimetic collagen scaffolds for human bone cell growth and differentiation. Tissue Eng 10(7-8):1148–1159. doi:10.1089/ten.2004.10.1148
11. Lee JY, Choi YS, Lee SJ, Chung CP, Park YJ (2011) Bioactive peptide-modified biomaterials for bone regeneration. Curr Pharm Des 17(25):2663–2676
12. Thorwarth M, Schultze-Mosgau S, Wehrhan F, Kessler P, Srour S, Wiltfang J, Andreas Schlegel K (2005) Bioactivation of an anorganic bone matrix by P-15 peptide for the promotion of early bone formation. Biomaterials 26(28):5648–5657. doi:10.1016/j.biomaterials.2005.02.023
13. Bhatnagar RS, Qian JJ, Wedrychowska A, Sadeghi M, Wu YM, Smith N (1999) Design of biomimetic habitats for tissue engineering with P-15, a synthetic peptide analogue of collagen. Tissue Eng 5(1):53–65
14. Mobbs RJ, Maharaj M, Rao PJ (2014) Clinical outcomes and fusion rates following anterior lumbar interbody fusion with bone graft substitute i-FACTOR, an anorganic bone matrix/P-15 composite. J Neurosurg Spine 21(6):867–876. doi:10.3171/2014.9.SPINE131151
15. Garrison KR, Donell S, Ryder J, Shemilt I, Mugford M, Harvey I, Song F (2007) Clinical effectiveness and cost-effectiveness of bone morphogenetic proteins in the non-healing of fractures and spinal

fusion: a systematic review. Health Technol Assess 11(30):1–150, iii-iv
16. Gibson S, McLeod I, Wardlaw D, Urbaniak S (2002) Allograft versus autograft in instrumented posterolateral lumbar spinal fusion: a randomized control trial. Spine 27(15):1599–1603
17. Arrington ED, Smith WJ, Chambers HG, Bucknell AL, Davino NA (1996) Complications of iliac crest bone graft harvesting. Clin Orthop Relat Res ((329):300-309
18. Banwart JC, Asher MA, Hassanein RS (1995) Iliac crest bone graft harvest donor site morbidity. A statistical evaluation. Spine 20(9): 1055–1060
19. Floyd T, Ohnmeiss D (2000) A meta-analysis of autograft versus allograft in anterior cervical fusion. Eur Spine J 9(5):398–403
20. Cahill KS, Chi JH, Day A, Claus EB (2009) Prevalence, complications, and hospital charges associated with use of bone-morphogenetic proteins in spinal fusion procedures. JAMA 302(1):58–66. doi:10.1001/jama.2009.956
21. Carragee EJ, Hurwitz EL, Weiner BK (2011) A critical review of recombinant human bone morphogenetic protein-2 trials in spinal surgery: emerging safety concerns and lessons learned. Spine J 11(6):471–491. doi:10.1016/j.spinee.2011.04.023
22. Hennessy KM, Pollot BE, Clem WC, Phipps MC, Sawyer AA, Culpepper BK, Bellis SL (2009) The effect of collagen I mimetic peptides on mesenchymal stem cell adhesion and differentiation, and on bone formation at hydroxyapatite surfaces. Biomaterials 30(10):1898–1909. doi:10.1016/j.biomaterials.2008.12.053
23. Li X, Contreras-Garcia A, LoVetri K, Yakandawala N, Wertheimer MR, De Crescenzo G, Hoemann CD (2015) Fusion peptide P15-CSP shows antibiofilm activity and pro-osteogenic activity when deposited as a coating on hydrophilic but not hydrophobic surfaces. J Biomed Mater Res A. doi:10.1002/jbm.a.35511
24. Kiely PD, Brecevich AT, Taher F, Nguyen JT, Cammisa FP, Abjornson C (2014) Evaluation of a new formulation of demineralized bone matrix putty in a rabbit posterolateral spinal fusion model. Spine J 14(9):2155–2163. doi:10.1016/j.spinee.2014.01.053
25. Eaton GJ, Zhang QS, Diallo C, Matsuzawa A, Ichijo H, Steinbeck MJ, Freeman TA (2014) Inhibition of apoptosis signal-regulating kinase 1 enhances endochondral bone formation by increasing chondrocyte survival. Cell Death Dis 5:e1522. doi:10.1038/cddis.2014.480
26. Myszka DG, Arulanantham PR, Sana T, Wu Z, Morton TA, Ciardelli TL (1996) Kinetic analysis of ligand binding to interleukin-2 receptor complexes created on an optical biosensor surface. Protein Sci 5(12):2468–2478. doi:10.1002/pro.5560051209
27. Hanks T, Atkinson BL (2004) Comparison of cell viability on anorganic bone matrix with or without P-15 cell binding peptide. Biomaterials 25(19):4831–4836. doi:10.1016/j.biomaterials.2003.12.007
28. Kubler A, Neugebauer J, Oh JH, Scheer M, Zoller JE (2004) Growth and proliferation of human osteoblasts on different bone graft substitutes: an in vitro study. Implant Dent 13(2):171–179
29. Fukumoto T, Sanyal A, Fitzsimmons JS, O'Driscoll SW (2002) Expression of beta1 integrins during periosteal chondrogenesis. Osteoarthritis Cartilage 10(2):135–144. doi:10.1053/joca.2001.0490
30. Kundu AK, Khatiwala CB, Putnam AJ (2009) Extracellular matrix remodeling, integrin expression, and downstream signaling pathways influence the osteogenic differentiation of mesenchymal stem cells on poly(lactide-co-glycolide) substrates. Tissue Eng Part A 15(2):273–283. doi:10.1089/ten.tea.2008.0055
31. Shih YR, Tseng KF, Lai HY, Lin CH, Lee OK (2011) Matrix stiffness regulation of integrin-mediated mechanotransduction during osteogenic differentiation of human mesenchymal stem cells. J Bone Miner Res 26(4):730–738. doi:10.1002/jbmr.278